

# Modeling and simulations of quantum phase slips in ultrathin superconducting wires

Andreas Andersson and Jack Lidmar\*

*Department of Theoretical Physics, KTH Royal Institute of Technology, AlbaNova, SE-106 91 Stockholm, Sweden*

(Dated: April 17, 2015)

We study quantum phase slips (QPS) in ultrathin superconducting wires. Starting from an effective one-dimensional microscopic model, which includes electromagnetic fluctuations, we map the problem to a (1+1)-dimensional gas of interacting instantons. We introduce a method to calculate the tunneling amplitude of quantum phase slips directly from Monte Carlo simulations. This allows us to go beyond the dilute instanton gas approximation and study the problem without any limitations of the density of QPS. We find that the tunneling amplitude shows a characteristic scaling behavior near the superconductor-insulator transition. We also calculate the voltage-charge relation of the insulating state, which is the dual of the Josephson current-phase relation in ordinary superconducting weak links. This evolves from a sinusoidal form in the regime of dilute QPS to more exotic shapes for higher QPS densities, where interactions are important.

PACS numbers: 74.78.-w, 74.40.-n, 74.50.+r, 74.78.Na

## I. INTRODUCTION

In ultrathin, effectively one-dimensional, superconducting wires the supercurrent may be degraded by phase slips, i.e., sudden unwindings of the phase of the superconducting order parameter. Thermal phase slips cause dissipation and in principle destroy superconductivity at any nonzero temperature. At zero temperature superconductivity may be disrupted instead by quantum phase slips (QPS) in which the phase unwinding occurs via quantum mechanical tunneling events. The possibility of observing QPS has received much attention recently.<sup>1–5</sup> In wires of finite length, incoherent QPS lead to a small resistivity even in the superconducting state. As the thickness of the wire is reduced, the QPS become more frequent and eventually drive the wire to an insulating state. In this regime, the QPS tunneling acts coherently to change the ground state to a state with the Cooper pairs immobilized. This state is characterized by a nontrivial voltage-charge relation, which is the dual of the Josephson current-phase relation occurring in tunnel junctions or weak links.<sup>6</sup> Evidence for coherent QPS was recently observed in wires,<sup>7,8</sup> and Josephson junction arrays.<sup>9</sup>

Superconducting fluctuations in a wire can be described using an effective action written in terms of the amplitude  $\Delta$  and phase  $\phi$  of the superconducting order parameter.<sup>10,11</sup> Quantum phase slips correspond to instantons of this action, which appear as vortex-like configurations of the phase. In the limit of dilute QPS the tunneling amplitude is determined by the action of single instantons,  $t_1 \sim e^{-S_{\text{QPS}}}$ . Phase slips are, however, nonlocal events, since they require a rearrangement of the phase over a large portion of the wire. This motivates the consideration of interactions between QPS, especially in the regime near the transition, where they become plentiful.

A phase slip is associated with the tunneling of flux across the wire, which gives rise to a voltage pulse. It is for this reason important to include also the fluctuations of the electromagnetic fields in the model.

The microscopic action of a superconducting wire which

includes these effects is rather complicated.<sup>10,11</sup> In this paper, we model QPS by transforming the action into a model, which is more manageable and suitable for numerical simulations and approximations. We also show how the QPS tunneling amplitude may be extracted from simulation data, and use this to study its dependence on microscopic parameters. Near the superconductor-insulator (SI) transition, it obeys a characteristic length dependence that can be used to locate the critical parameters. Finally, we calculate the characteristic response of the wire, in the insulating regime of coherent QPS, to an imposed charge displacement. Similar physics occurs also in discrete Josephson junction chains.<sup>4,9,12–15</sup>

The paper is organized as follows: In Sec. II, we map an effective microscopic action to a dual action describing a (1+1)D gas of interacting QPS. This reformulation is crucial and lays the foundation for Sec. III, where we introduce an approach to calculate the tunneling amplitude and the low-energy band relation for QPS. Section IV summarizes the grand canonical Monte Carlo method we use to simulate the system described by our dual action. In Sec. V, we present and discuss results from the simulations.

## II. MODELS OF SUPERCONDUCTING WIRES

Our starting point is a microscopic effective action for thin homogenous superconducting wires in the dirty limit, derived by Golubev and Zaikin.<sup>10</sup> The wires are assumed to be made of conventional *s*-wave superconductors, well described by BCS theory. Well below the bulk superconducting temperature the fermions are gapped and may be integrated out resulting in a purely bosonic action, which is subsequently averaged over short range disorder, assuming a mean free path  $l$  (typically  $\sim 5 - 15\text{nm}$ ) much smaller than the superconducting coherence length of the clean system  $\xi_0 \sim \hbar v_F / \pi \Delta$  ( $\sim 0.1 - 1\mu\text{m}$ ). We will limit the present discussion to relatively homogenous wires with no long range disorder on scales larger than

the coherence length  $\xi \sim \sqrt{l\xi_0}$ , although such disorder might lead to interesting phenomena, e.g., suppression of QPS by Aharonov-Casher interference effects<sup>12</sup> or Cooper pair localization.<sup>16</sup> The result is a phase-only theory with a constant amplitude  $\Delta_0$ , except in the QPS cores (of size  $\sim \xi$ ) where it will have to momentarily vanish. In particular, the gap is assumed to remain finite across the SI transition, where phase coherence is lost. We here assume the absence of strong pair breaking interactions, which might otherwise close the fermion gap before the phase fluctuations destroys superconductivity.<sup>17</sup>

In this section, we map this action, first to a dual charge-current model, and then to a (1+1)D gas of interacting QPS, paying special attention to the electromagnetic field. The resulting model is similar to a 2D Coulomb gas, but with a slightly more complicated interaction. We would like to study the QPS occurring in the bulk of the wire and therefore use periodic boundary conditions to avoid boundary effects. The geometry of the system is thus a loop, but we will consider it large enough that we may neglect the effect of the geometric loop inductance  $L_G$ , see Fig. 1(a) and (b). Under these conditions, a QPS event corresponds to the tunneling of a flux quantum across the wire, in or out of the loop. In the limit of very large geometric loop inductance  $L_G \rightarrow \infty$ , the magnetic energy  $\Phi^2/2L_G$  becomes negligible and the flux through the loop may fluctuate in time. As shown below, this fact also relaxes the neutrality constraint usually present in a 2D Coulomb gas, and allows configurations with a nonzero net number of instantons. This point will be important in what follows.

One may consider the geometry chosen more as a theoretical tool to be able to extract the bulk properties of a wire. It is straightforward to also consider smaller loops with non-negligible loop inductance, or straight wires with boundaries. A common setup is, e.g., to consider a small nanoring threaded by half a flux quantum, see Fig. 1(c) and (d).<sup>12,13,18,19</sup> In absence of QPS there are then only two degenerate ground states, with differing fluxoid states, corresponding to clockwise and anticlockwise persistent currents. Such geometries have recently provided evidence for coherent QPS in experiments.<sup>7-9</sup> The tunneling amplitude in this geometry is not expected to differ appreciably from the one calculated below, in which the geometric loop inductance is considered infinite.

In general we use units where  $\hbar = 1$ , although in some equations it is reinstated for clarity.

### A. Microscopic effective action

The imaginary time action derived in Refs. 10 and 11 for a wire with cross section  $s$  is given by

$$S = \int \frac{d\omega}{2\pi} \frac{dk}{2\pi} \left\{ \frac{C}{2} V^2 + \frac{s\chi_D}{2} |E|^2 + \frac{s\chi_J}{2(2e)^2} |-i\omega\phi - 2eV|^2 + \frac{s\chi_L}{8m^2} |ik\phi + 2eA|^2 + \frac{s\chi_\Delta}{2} |\delta\Delta|^2 \right\} \equiv S_\phi + S_\Delta. \quad (1)$$

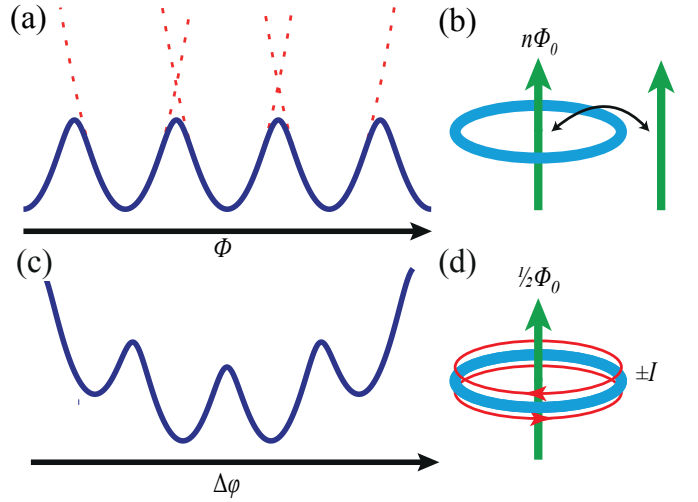


FIG. 1. (Color online) (a) Energy vs flux for a closed loop when the loop inductance is very large or infinite. In absence of tunneling all states with integer number of flux quanta are degenerate, while the tunneling process illustrated in (b) lifts this degeneracy. (c) shows the opposite situation of a small ring with small loop inductance, threaded by half a flux quantum. There is then just a twofold ground state degeneracy with different fluxoid number  $n = \oint (d\phi/dx) dx / 2\pi$ . The tunneling process sketched in (d) connects these two states having opposite circulation of the current. (a), (b) correspond to the situation modeled in the present work.

Here  $\phi$  and  $\Delta = \Delta_0 + \delta\Delta$  are the phase and amplitude of the superconducting order parameter  $\psi = \Delta e^{i\phi}$ , respectively. Importantly, the action includes also the electromagnetic field fluctuations via the vector potential  $A$ , the voltage  $V$ , and the electric field  $E = -ikV - i\omega A$ . The Coulomb interaction is parametrized by the capacitance per length  $C$ . The geometric inductance of the wire is in general much smaller than the kinetic one and has been neglected. This bosonic action is obtained from an expansion of an ordinary BCS action around the low temperature mean field solution  $\Delta_0$ , after the fermions have been integrated out. The wire diameter is assumed to be less than the superconducting coherence length  $\xi \approx \sqrt{D/\Delta_0}$ , thereby justifying a purely one-dimensional description. The kernels  $\chi_i$  are given by<sup>10,11</sup>

$$\chi_\Delta = 2N_0 \left( 1 + \frac{\omega^2}{12\Delta_0^2} + \frac{\pi D k^2}{8\Delta_0} \right), \quad (2)$$

$$\chi_J = 2e^2 N_0 \left( 1 - \frac{\omega^2}{6\Delta_0^2} - \frac{\pi D k^2}{8\Delta_0} \right), \quad (3)$$

$$\chi_L = 2\pi m^2 N_0 D \Delta_0, \quad (4)$$

$$\chi_D = \frac{\pi e^2 N_0 D}{4\Delta_0}, \quad (5)$$

in the limit of low  $\omega$ ,  $Dk^2 \ll \Delta_0$ , where  $\Delta_0$  is the superconducting gap,  $N_0$  the density of states at the Fermi level,  $D = v_F l / 3$  is the diffusion coefficient,  $v_F$  the Fermi velocity, and  $l$  the mean free path.

The action has two parts,  $S = S_\Delta + S_\phi$ , describing amplitude and phase fluctuations, respectively. The phase action allows both for smooth spin-wave fluctuations and instantons, which are singular vortex-like configurations, where the phase winds by a multiple of  $2\pi$  as the singularity is encircled. The latter ones are responsible for the QPS. At the center of a QPS the amplitude  $\Delta$  of the superconducting order parameter has to go to zero, thereby providing a short distance cutoff for the otherwise divergent phase contribution. The large variation of  $\Delta$  inside the core thus effectively couples the phase and amplitude fluctuations, despite the fact that they appear uncoupled to quadratic order in Eq. (1). The action  $S_{\text{QPS}}$  of such instanton configurations determines to a large extent the QPS tunneling amplitude. It has a local core part  $S_{\text{core}}$ , coming from the depletion of the amplitude  $\Delta$  at the centers, and an outer “hydrodynamic” part  $S_\phi$  from the phase variation surrounding the cores.

In what follows, we will estimate these contributions separately, starting with a reformulation of the phase contribution. Further on, we will study effects of interactions among the QPS.

### B. Dual action

As a first step let us introduce the new fields  $\mathbf{J} = (\rho, J)$ , where  $-2e\rho$  is the electric charge density and  $-2eJ$  the electric current, which should be integrated over in the partition function. By a Hubbard-Stratonovich transformation, we get

$$S_\phi = \int \frac{d\omega}{2\pi} \frac{dk}{2\pi} \left\{ \frac{C}{2} V^2 + \frac{s\chi_D}{2} |E|^2 + \frac{(2e)^2}{2s\chi_J} |\rho|^2 + \frac{4m^2}{2s\chi_L} |J|^2 + i\rho^*(-i\omega\phi - 2eV) + iJ^*(ik\phi + 2eA) \right\}, \quad (6)$$

where  $\rho^*(\omega, k) = \rho(-\omega, -k)$ , and similarly for  $J^*$ . We then split the phase field  $\phi = \phi_r + \phi_s$  into a regular and a singular piece. The singular part obeys

$$(\partial_x \partial_\tau - \partial_\tau \partial_x) \phi_s = 2\pi v(x, \tau), \quad (7)$$

where

$$v(x, \tau) = \sum_i v_i \delta(x - x_i) \delta(\tau - \tau_i), \quad v_i = \pm 1 \quad (8)$$

describes density of the phase slips, i.e., vortex-like configurations in the phase field  $\phi(x, \tau)$ . Integrating over the regular part  $\phi_r$  leads to the constraint  $\nabla \cdot \mathbf{J} = \partial_x J + \partial_\tau \rho = 0$ , of charge conservation. This can be resolved by representing the current as

$$\mathbf{J} = (\rho, J) = (-\partial_x q, \partial_\tau q) \quad (9)$$

or in Fourier space  $\mathbf{J} = (-ikq, -i\omega q)$ , where  $q(x, \tau)$  is a dimensionless continuous charge field representing the

charge passing through a point  $x$  in the wire, leading to an action

$$S_\phi = \int \frac{d\omega}{2\pi} \frac{dk}{2\pi} \left\{ \frac{C}{2} V^2 + \frac{s\chi_D}{2} |E|^2 + \frac{(2e)^2}{2s\chi_J} |kq|^2 + \frac{4m^2}{2s\chi_L} |\omega q|^2 + iq(-\omega, -k)(2\pi v(\omega, k) - 2eE(\omega, k)) \right\}. \quad (10)$$

Since the action is quadratic in both the voltage  $V$  and the vector potential  $A$ , these can be integrated out exactly. We neglect here any spatial variations in the vector potential  $A$ , i.e., we treat it as spatially global but time dependent,  $A = A(\tau)$ . Fluctuations in  $A$  are thus considered instantaneous, an approximation which is justified because of the high speed of light and the length of realistic wires,  $c \gg L\Delta/\hbar$ . Performing the integrations over  $V$  and  $A$ , substituting Eqs. (3)-(5), and expanding  $1/\chi_J$  to lowest order for small  $\omega$  and  $k$  obtains an action which can be expressed as

$$S_\phi = \int \frac{d\omega}{2\pi} \frac{dk}{2\pi} \left\{ \frac{(2e)^2}{2} \left( \tilde{L}(k) \omega^2 + \frac{1}{\tilde{C}(k)} k^2 + 2\pi\delta(kL) \frac{1}{C\lambda^2} \right) |q(\omega, k)|^2 + 2\pi iq(-\omega, -k)v(\omega, k) \right\}, \quad (11)$$

where we introduced the kinetic inductance  $\tilde{L}(k)$  and an effective capacitance  $\tilde{C}(k)$  (both per unit length) given by

$$\tilde{L}(k) = \frac{1}{\pi\sigma\Delta_0 s} \left( 1 + \frac{\pi D k^2}{6\Delta_0} \right), \quad (12)$$

$$\frac{1}{\tilde{C}(k)} = \frac{D}{\sigma s} \left( 1 + \frac{\pi D k^2}{8\Delta_0} \right) + \frac{1}{C} \frac{1}{1 + \lambda^2 k^2}, \quad (13)$$

$$\lambda^2 = \frac{\pi\sigma s}{8\Delta_0 C}, \quad (14)$$

where  $\sigma = 2e^2 N_0 D$  is the normal state Drude conductivity and  $\lambda$  is a screening length for the charge carriers. The term proportional to  $\delta(k)$  in Eq. (11) results from the integration over the spatially constant vector potential  $A(\omega)$ .

For realistic parameters of experimental wires, the geometric capacitance per length  $C$  is small,  $C \ll 2e^2 N_0 s = \sigma s/D$ . Accordingly, we drop the first term in Eq. (13) in this limit. This also means that  $\lambda \gg \xi \simeq \sqrt{D/\Delta_0}$ , where  $\xi$  is the coherence length. For low  $k \ll \lambda^{-1}$  we get the velocity of the Mooij-Schön mode<sup>20</sup>

$$c_0 = 1/\sqrt{\tilde{L}C} = \sqrt{\pi\sigma\Delta_0 s/C}. \quad (15)$$

The terms which are of higher order in  $k$  in Eqs. (12)-(13) become large when  $Dk^2/\Delta_0 \sim 1$ , i.e., on length scales short compared to  $\xi$ , which serves as a short distance cutoff in the model. Below this cutoff, it is convenient to write the action as

$$S_\phi = \frac{1}{\beta L} \sum_{k, \omega} \frac{1}{2Kc_0} \left\{ (\omega^2 + \epsilon^2(k)) |q(\omega, k)|^2 + 2\pi iq(-\omega, -k)v(\omega, k) \right\}, \quad (16)$$

where we omitted the terms of order  $Dk^2/\Delta_0$ , and also introduced infrared cutoffs by considering a wire of finite length with periodic boundary conditions (i.e., a large loop), at finite temperature  $\beta^{-1}$ . The sum goes over  $\omega = 2\pi m/\beta$ ,  $k = 2\pi n/L$ , with  $m, n \in \mathbb{Z}$ . The action has a dispersion

$$\epsilon(k) = \frac{c_0 k}{\sqrt{1 + \lambda^2 k^2}} + \delta_{k,0} \frac{c_0}{\lambda}, \quad (17)$$

with a coupling constant

$$K = \frac{\sqrt{\pi\sigma s\Delta_0 C}}{(2e)^2} = \frac{1}{(2e)^2} \sqrt{\frac{C}{\tilde{L}}} = \frac{R_Q}{2\pi Z}, \quad (18)$$

where  $\sqrt{\tilde{L}/C} = Z$  is the impedance of the wire and  $R_Q = h/4e^2$  the resistance quantum.

Although the action in Eq. (16) was derived from a microscopic theory, a similar action could be written down on phenomenological grounds, i.e., as the action of a superconducting transmission line with a linear dispersion modified by the typically large charge screening length  $\lambda$ .

In the above equations, we assumed that  $\lambda \gg \xi$ . In the opposite limit  $\lambda \ll \xi$ , Eq. (16) remains a valid parametrization of the action, but with different parameters

$$\tilde{K} = N_0 s \sqrt{\pi D \Delta_0}/2, \quad \tilde{c}_0 = \sqrt{\pi D \Delta_0}, \quad (19)$$

and a linear dispersion  $\epsilon(k) = \tilde{c}_0 k + \delta_{k,0} \Delta_0/\sqrt{8}$ , while the intermediate regime  $\lambda \sim \xi$  is described by Eq. (11). Note also that for a discrete Josephson junction array one obtains a similar action, but with

$$K = \sqrt{E_J/E_{C_0}}, \quad c_0 = \sqrt{E_J E_{C_0}}, \quad \lambda = \sqrt{C/C_0}, \quad (20)$$

where  $E_J$  is the Josephson coupling energy,  $E_{C_0} = (2e)^2/C_0$ , and  $C, C_0$  the capacitance of the junctions and to ground, respectively.

From Eq. (11) or (16), one can proceed in two ways: Sum over the instanton fluctuations  $v(x, \tau)$  to get a sine-Gordon-like action solely in terms of the charge displacement  $q(x, \tau)$ ,

$$S[q] = S_1[q] - \iint 2y \cos(2\pi q(x, \tau)) \frac{dx d\tau}{x_0 \tau_0}, \quad (21)$$

where  $S_1$  is the quadratic part of the action (i.e., the first line of Eq. (16)) and  $y$  the QPS “fugacity” (see below). Or one can integrate over the  $q$ -field to get an effective action for the quantum phase slips. We will do the latter here since this gives a model which can be studied using Monte Carlo simulations relatively easy.

### C. Instanton gas

Performing the functional integration over the charge field  $q(x, \tau)$  in (11) or (16) maps the problem to a (1+1)D

gas of interacting instantons, with an action

$$S_v = \frac{(2\pi)^2 K c_0}{2\beta L} \sum_{k, \omega} \frac{1}{\omega^2 + \epsilon^2(k)} |v(\omega, k)|^2 \\ = \frac{1}{2} \sum_{\{i, j\}} v_i V(x_i - x_j, \tau_i - \tau_j) v_j, \quad (22)$$

where  $v_i = \pm 1$  denotes the topological charge (vorticity) of the instantons located at  $(x_i, \tau_i)$  and we introduced the pair interaction  $V(x, \tau)$ . The summation also needs to be cut off at high  $\omega, k$ , where the effective action derived here is no longer applicable. We here use a Gaussian cutoff, giving an interaction

$$V(x, \tau) = \frac{(2\pi)^2 K c_0}{\beta L} \sum_{k, \omega} \frac{e^{ikx - i\omega\tau}}{\omega^2 + \epsilon^2(k)} e^{-\frac{1}{2}(kx_0)^2 - \frac{1}{2}(\omega\tau_0)^2}. \quad (23)$$

A natural choice for the ultraviolet cutoffs in space and time are

$$x_0 = \sqrt{\pi D/8\Delta_0} \approx \xi, \quad \tau_0 \approx 1/\sqrt{8\Delta_0}, \quad (24)$$

so that  $\lambda = c_0 \tau_0$ . (This choice also gives  $\tilde{c}_0 = x_0/\tau_0$ ,  $\tilde{K} = K c_0/\tilde{c}_0 = K \lambda/x_0$ .)

The problem now has the form of a classical 2D gas of interacting charges with a partition function

$$Z = \sum_{N=0}^{\infty} \frac{y^N}{N!} \int \prod_{i=1}^N \frac{dx_i d\tau_i}{x_0 \tau_0} \sum_{v_i=\pm 1} e^{-S_v}. \quad (25)$$

The core contribution  $S_{\text{core}}$  enters the fugacity,<sup>10,11</sup>

$$y \approx S_{\text{core}} e^{-S_{\text{core}}}. \quad (26)$$

Note that the  $k = 0$  contribution in Eq. (17) removes the zero mode in the dispersion and thereby renders the single instanton action  $\frac{1}{2}V(0, 0)$  finite. As a result, the partition function includes configurations with no restriction on the net number of instantons.

### D. QPS interaction

The QPS interaction in Eq. (23) does not allow for an exact analytic solution, due to the added complication of the charge screening length  $\lambda$ . However, on length scales much larger than  $\lambda$  the interaction is purely logarithmic in space-time  $V(x, \tau) \sim \pi K \ln[(x^2 + c_0^2 \tau^2)/\lambda^2]$ , i.e., in the limit  $\lambda \ll x \ll L$ , the model is essentially equivalent to the 2D Coulomb gas. Examples of the general behavior for finite systems are displayed in Fig. 2, for different values of  $\lambda$ .

Of particular interest is the self-interaction  $V_0 = V(0, 0)$  in a finite system of length  $L$ . In the limit  $\beta/\tau_0 \gg 1$ , this can be approximated as

$$V_0 \approx 2\pi \tilde{K} \ln(L/x_0), \quad (L \gg x_0 \gg \lambda) \quad (27a)$$

$$V_0 \approx 2\pi K \ln(L/\lambda) + bK\lambda/x_0, \quad (L \gg \lambda \gg x_0) \quad (27b)$$

$$V_0 \approx bK\lambda/x_0, \quad (\lambda \gg x_0, L) \quad (27c)$$

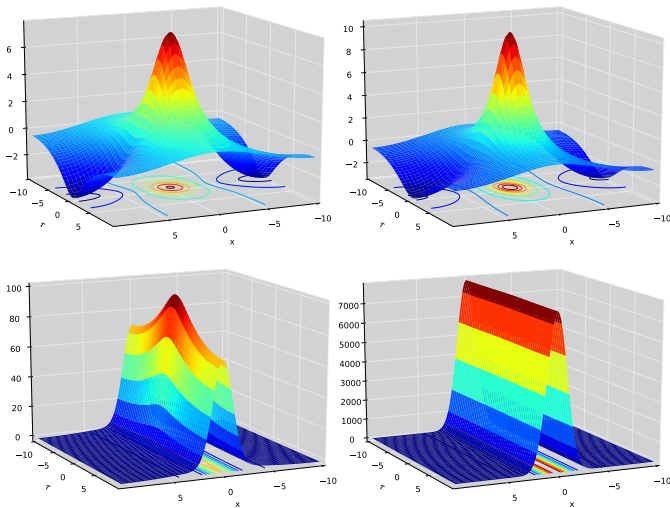


FIG. 2. (Color online) The vortex interaction  $V(x, \tau)$  for some different values of the parameter  $\lambda$ . From left to right, top to bottom, the values are  $\lambda = 0.01, 1.0, 10$ , and  $100$ . System size is  $20 \times 20$ ,  $K = 1.0$ , and  $c_0 = 1$ . Increasing  $c_0$  more, squeezes the potential in the  $\tau$  direction, making it more anisotropic in space-time.

where  $b$  is a constant whose precise value depends on the implementation of the cutoff. Using Eq. (23) we estimate  $b \approx 0.5\sqrt{2\pi^3} \approx 4$ .

### E. Core action

At the center of a QPS, the amplitude  $\Delta$  of the superconducting order parameter has to go to zero, thereby providing a cutoff for the otherwise divergent phase contribution. The core part of the action is

$$S_{\Delta} = \int \frac{d\omega}{2\pi} \frac{dk}{2\pi} \frac{s\chi_{\Delta}}{2} |\delta\Delta|^2 = \int \frac{d\omega}{2\pi} \frac{dk}{2\pi} N_0 s \left( 1 + \frac{\omega^2}{12\Delta_0^2} + \frac{\pi D k^2}{8\Delta_0} \right) |\delta\Delta|^2. \quad (28)$$

The typical length and time scales for variations of  $\delta\Delta$  are set by the coherence length  $\xi$  and the inverse gap  $1/\Delta_0$ .

Following Refs. 10 and 11 we may estimate the core contribution using a Gaussian profile  $\delta\Delta(x, \tau) = \Delta_0 e^{-x^2/2x_0^2 - \tau^2/2\tau_0^2}$ , or in Fourier space  $\delta\Delta(\omega, k) = 2\pi\Delta_0 x_0 \tau_0 e^{-k^2 x_0^2/2 - \omega^2 \tau_0^2/2}$ . Carrying out the integration gives

$$S_{\text{core}} = \pi N_0 \Delta_0^2 s x_0 \tau_0 \left( 1 + \frac{1}{24\Delta_0^2 \tau_0^2} + \frac{\pi D}{16\Delta_0 x_0^2} \right), \quad (29)$$

and substituting  $x_0, \tau_0$  by Eq. (24) for consistency,

$$S_{\text{core}} = a \frac{K\lambda}{x_0}, \quad (30)$$

where  $a = 11\pi/24 \approx 1.44$  is a numerical factor. The precise value of  $a$  depends on the assumed profile and neglected higher order terms in the action. Note that the total cost of inserting one QPS in the system consists of the core action Eq. (30) and (half) the self-interaction (27). The latter contains in addition to the logarithmic length dependence a constant part  $\sim bK\lambda/x_0$  with the same parametric dependence on microscopic parameters as the core part. Our estimates suggest that they are comparable in magnitude,  $a \approx 1.44$  and  $b/2 \approx 2$ . In principle these estimates might be improved on by optimizing the total action cost with regard to the cutoffs.<sup>10,11</sup> This would, however, only have a minor effect on the numerical estimates, which are anyhow quite uncertain. In contrast to previous work,<sup>10,11</sup> our estimates of  $x_0$  and  $\tau_0$  remain parametrically the same also when  $\lambda < x_0$ .

In total the local action for one QPS becomes  $S_0 = cK\lambda/x_0$ , with  $c = a + b/2 \approx 3.44$ . In terms of experimentally accessible parameters,

$$S_0 = c\sqrt{2}N_0 s \xi \Delta_0 = \frac{c}{4\sqrt{2}} \frac{R_Q}{R_N} \frac{L}{\xi}, \quad (31)$$

where  $R_N = L/\sigma s$  is the normal state resistance.

## III. QUANTUM PHASE SLIP AMPLITUDE

### A. Reduction to zero-dimensional model

In this section we will describe a method (similar to one employed in a different context in Refs. 21 and 22) to calculate the tunneling amplitude of QPS using the action obtained above. We will do this by reducing the model to a low energy effectively zero-dimensional model, treating the whole wire as a lumped element.

As discussed, the instantons or QPS correspond to tunneling events where the phase slips by  $2\pi$ . In order to calculate the tunneling amplitude of such QPS, it is convenient, although not essential, to consider a wire with periodic boundary conditions, i.e., a closed loop. If we neglect any self-inductance of the loop, the ground-state energy of the system is periodic in the flux  $\Phi$  going through the loop with period  $\Phi_0$ , see Fig. 1. A quantum phase slip then is accompanied with the tunneling of a flux quantum  $\Phi_0$  in or out of the loop, which will generate a voltage pulse. Thus we consider the flux  $\Phi = LA$  as a dynamical variable. In the absence of tunneling, the ground states with  $n$  integer flux quanta are all degenerate. Tunneling will lift this degeneracy. At low energies, the whole system can be described by the effective tight-binding Hamiltonian<sup>12</sup>

$$H = \sum_n \tilde{E}_0 |n\rangle \langle n| - \sum_{n,m} t_m (|n+m\rangle \langle n| + |n\rangle \langle n+m|), \quad (32)$$

where  $\tilde{E}_0$  is the ground state energy without tunneling and  $t_m$  are transition amplitudes for the simultaneous tunneling of  $m$  flux quanta. Deep in the superconducting phase, where these tunneling events are rare, the dominating transitions should be for  $m = \pm 1$ , but in general also other transition amplitudes may be important.<sup>23</sup> Due to the translation invariance of the index  $n$ , the eigenstates of this Hamiltonian are plane waves:

$$|k\rangle = \frac{1}{\sqrt{N}} \sum_n e^{ikn} |n\rangle, \quad (33)$$

with energies

$$E_k = \tilde{E}_0 - \sum_{m=1}^N 2t_m \cos km, \quad 0 \leq k < 2\pi, \quad (34)$$

where, for normalization purposes, we have limited the number of flux states to  $N$ , but eventually this limitation will be removed.

Our goal here is to relate the tunneling amplitudes  $t_m$  to the properties of the models formulated in the previous section. A crucial ingredient in those is the inclusion of electromagnetic fluctuations, which lifts the neutrality constraint in the instanton gas formulation. Consider now the partition function  $Z_m$  restricted to configurations where the number of instantons and anti-instantons differ by exactly  $m$  ( $m = \sum_i v_i$  is thus the net vorticity). In the language of quantum mechanics this corresponds to a matrix element

$$Z_m = \langle n+m | e^{-\beta H} | n \rangle, \quad (35)$$

which starts from a state  $n$  at  $\tau = 0$ , evolves in imaginary time, and ends in  $n+m$  at  $\tau = \beta$ . This allows us to calculate

$$\begin{aligned} e^{-\beta E_k} &= \langle k | e^{-\beta H} | k \rangle = \frac{1}{N} \sum_{n,n'} \langle n' | e^{-\beta H} | n \rangle e^{ik(n-n')} \\ &= \frac{1}{N} \sum_{n,m} \langle n+m | e^{-\beta H} | n \rangle e^{ikm} = \sum_m Z_m e^{ikm}. \end{aligned} \quad (36)$$

Denoting  $E_k - E_0 = \Delta E_k$ , we get

$$e^{-\beta \Delta E_k} = \frac{\sum_m Z_m e^{ikm}}{\sum_m Z_m} = \langle e^{ikm} \rangle. \quad (37)$$

In a simulation, it is easy to calculate the average  $\langle e^{ikm} \rangle$  by first collecting the histograms  $Z_m$  of  $m = \sum_i v_i$ . From the low-energy eigenstates  $E_k$  calculated using Eq. (37), we can then obtain the tunneling amplitudes, using Eq. (34), as

$$t_m = - \int_0^{2\pi} \frac{dk}{2\pi} \Delta E_k e^{-ikm}. \quad (38)$$

Note that an implicit assumption in this derivation is the low-temperature limit  $\beta \rightarrow \infty$ . In practice the  $t_m$  and  $E_k$  saturate quickly to constants as  $\beta \gtrsim L/c_0$ .

## B. Voltage-charge relation

The low-energy band relation Eq. (34) and its derivatives are important characteristics of the QPS lumped element. The  $k$  in this relation corresponds, up to a factor  $2e/2\pi$ , precisely to an externally imposed charge displacement  $D$ . Indeed, adding a source term  $i \int D E dx = \int D \dot{A} dx$  [with  $D = (2e/2\pi)k$ ] to the action Eq. (1) and going through the transformations up to (22) leads to an additional term  $i(2\pi/2e)D \sum_i v_i = ikm$  in the latter.  $E_k$ , defined via Eq. (37), therefore gives the energy dependence of the QPS element on an induced charge. The first derivative gives the voltage drop

$$V_k = \frac{2\pi}{2e} \frac{\partial E_k}{\partial k} = \frac{2\pi}{2e} \sum_m 2t_m m \sin km \quad (39)$$

along the wire as a function of the charge displacement. The second derivative

$$C_k^{-1} = \left( \frac{2\pi}{2e} \right)^2 \frac{\partial^2 E_k}{\partial k^2} = \left( \frac{2\pi}{2e} \right)^2 \sum_m 2t_m m^2 \cos km \quad (40)$$

gives the inverse effective capacitance of the wire. The linear response of the system for  $k = 0$  is thus capacitive in the presence of QPS. Under voltage biased conditions no current will flow below the threshold voltage  $V_{\text{thr}} = \max_k V_k$ .

In the regime of coherent QPS, the system is characterized by a  $2e$ -periodic voltage-charge displacement relation (39), which is the dual analog of the Josephson current-phase relation  $I = I_c \sin \gamma$  of the superconducting phase. When  $m = 1$  dominates,  $V(k)$  reduces to a sinusoidal form, but in general it may be more complicated.

## C. Dilute QPS limit

When interactions between the instantons are neglected the method discussed in Sec. III A reproduces a standard instanton calculation in the dilute instanton gas approximation. Let us consider the partition function for phase slips in Eq. (25) in this limit and calculate the QPS amplitude. With  $N_+$  instantons and  $N_-$  anti-instantons with fugacity  $\tilde{y} = S_{\text{core}} \exp(-S_{\text{core}} - \frac{1}{2}V_0)$  the partition function becomes

$$Z = \sum_{N_+, N_-} \frac{\tilde{y}^{N_+} \tilde{y}^{N_-}}{N_+! N_-!} \Omega^{N_+} \Omega^{N_-} = e^{2\tilde{y}\Omega}. \quad (41)$$

The variable  $\Omega = (L\beta/x_0\tau_0)$  is the system volume in space-time. From here, the desired average  $\langle e^{ikm} \rangle = \langle e^{ik(N_+ - N_-)} \rangle$  is easily calculated

$$\begin{aligned} \langle e^{ikm} \rangle &= \frac{1}{Z} \sum_{N_+, N_-} \frac{\tilde{y}^{N_+} \tilde{y}^{N_-}}{N_+! N_-!} \Omega^{N_+} \Omega^{N_-} e^{ik(N_+ - N_-)} \\ &= e^{\tilde{y}\Omega(e^{ik} + e^{-ik} - 2)} = e^{-2\tilde{y}\Omega(1 - \cos k)}. \end{aligned} \quad (42)$$

This result gives directly

$$\Delta E_k^{\text{DL}} = \frac{2L\tilde{y}}{x_0\tau_0}(1 - \cos k). \quad (43)$$

In the dilute instanton limit the QPS amplitude therefore becomes

$$\begin{aligned} t_1^{\text{DL}} &= \frac{L\tilde{y}}{x_0\tau_0} = \frac{LS_{\text{core}}}{x_0\tau_0} e^{-S_{\text{core}} - \frac{1}{2}V_0} \\ &\approx 0.72\Delta_0 \frac{L}{\xi} \frac{R_Q L}{R_N \xi} e^{-S_{\text{core}} - \frac{1}{2}V_0}, \end{aligned} \quad (44)$$

with  $S_{\text{core}}$  and  $V_0$  given in Eq. (30) and (27), while  $t_m = 0$  for  $m > 1$ . This implies a purely sinusoidal voltage-charge relation  $V_k = V_c \sin k$ , and quantum capacitance  $C_k^{-1} \sim \cos k$ . Conversely, a nonsinusoidal relation is a signature of interactions among the QPS.

#### D. Superconductor-insulator transition

At low instanton densities the response of the wire is mostly superconducting with only a small resistance originating from incoherent QPS. As the density increases the proliferation of coherent QPS will drive the wire into an insulating state. The resulting SI transition has been studied both theoretically and experimentally in homogeneous nanowires<sup>1-3,5,10,11,24-26</sup> and in discrete Josephson junction chains.<sup>13-15,27,28</sup> An alternative scenario for the SI transition, not directly involving QPS, has also been proposed for nanowires with strong pair breaking interactions.<sup>17</sup>

The density of QPS is controlled mainly by two parameters appearing in the instanton action Eqs. (27) and (30), the local contribution  $S_0 \sim K\lambda/\xi$  and the logarithmic term  $\sim K \ln L/\lambda$ . In the thermodynamic limit  $L \rightarrow \infty$ ,  $\beta \rightarrow \infty$  the latter dominates, and may cause the system to undergo a Berezinskii-Kosterlitz-Thouless (BKT) transition.<sup>29</sup> The logarithmic interaction between the instantons on long length and time scales  $x \gg \lambda$ ,  $\tau \gg \lambda/c_0 \sim 1/\Delta_0$  is similar to a 2D Coulomb gas. For high values of  $K$  the instantons are all bound in neutral pairs and the system is in a superconducting state. As  $K$  is decreased below a critical value  $K_c = 2/\pi$ , the cost for adding an instanton eventually becomes less than the gain in entropy, and the proliferation of QPS drives the superconducting wire into an insulating state.

Note that this quantum phase transition is sharp only in the thermodynamic limit  $L \rightarrow \infty$ . For wires of finite length, several quantities acquire a length dependence characteristic of the transition. From Eq. (32), the QPS amplitudes  $t_m$  have the dimension of energy. General scaling arguments at a quantum phase transition<sup>30</sup> therefore suggest that  $t_1 \sim L^{-z}$ , where  $z$  is the dynamic critical exponent. As the BKT transition is isotropic in space-time,  $z = 1$ .

At very low densities,  $t_1$  is given by the approximation in Eq. (44), which can be combined with the expansion of

the self-interaction in the same limit in Eq. (27) to give

$$t_1^{\text{DL}} \sim L^{1-\pi K}. \quad (45)$$

At the critical coupling  $K = 2/\pi$  we have  $t_1^{\text{DL}} \sim L^{-1}$ , and so the suggested scaling of  $t_1$  holds here. Going beyond the dilute limit, interactions among the QPS will renormalize both  $K$  and  $y$ , and the actual transition will happen at a  $K_c > 2/\pi$  when the fully renormalized coupling  $K_R = 2/\pi$ .

Away from the dilute limit the transition can be studied using simulations instead. The critical value  $K_c$  can then be determined from the intersection of the curves  $Lt_1$  vs  $K$ , plotted for different  $L$  (see below).

The finite size scaling of  $t_1$  near the real transition should, by an argument similar to Ref. 31, be subject to a multiplicative logarithmic correction, so that

$$t_1(K_c) \sim L^{-1}/\ln(L/L_0). \quad (46)$$

The correction arises because  $t_1$  is proportional to the fugacity  $y$  [see Eq. (44)], which renormalizes logarithmically towards zero on approaching the fixed point of the transition:

$$t_1(K_c, y, L) = L^{-z} t_1(K_R, y'(L), 1) \sim L^{-1} y'(L). \quad (47)$$

It should be noted that in finite systems various crossovers are possible, and may in practice mask the real transition. In particular, the QPS interactions are logarithmic only on length scales  $\gg \lambda$  and thus it requires wires with  $L \gg \lambda$ . Although quite uncertain, the screening length can be estimated to be very large in most experimental wires, perhaps 100–1000 nm, unless special measures are taken to reduce it. In this case, the QPS amplitude is dominated by the exponential dependence on  $S_0 \sim K\lambda/\xi \sim R_Q L/R_N \xi$ , which may still lead to a rather sharp crossover from superconducting to insulating behavior.

#### IV. SIMULATION METHODS

The instanton gas formulation of Sec. II C is well suited for simulations. Since the number of instantons is fluctuating, a grand canonical Monte Carlo (MC) method is employed. We use a variant of the scheme developed by Lidmar and Wallin,<sup>32</sup> which in turn is an extension of an algorithm by Valleau and Cohen.<sup>33</sup> In brief, our algorithm consists of five different MC moves: (1) Creation of a single particle. (2) Destruction of a randomly chosen single particle. (3) Creation of a neutral pair of particles placed within a distance  $d$  from each other. (4) Destruction of a randomly chosen neutral pair of particles within a distance  $d$  from each other. (5) Displacement of a randomly chosen particle by a random distance in the interval  $(0, d)$ . The maximum displacement and pair distance  $d$  is arbitrary and can be tuned to optimize convergence (here we set  $d = 2x_0$ ). More details and a



derivation of the acceptance ratios for the creation and destruction moves can be found in Ref. 32.

We define an MC sweep to consist of  $L\beta/x_0\tau_0$  attempts of any of the four creation or destruction moves described above, with equal probability of 1/8, or the displacement move with probability 1/2. The system is typically equilibrated for  $10^5$  to  $10^6$  MC sweeps, after which we sample during  $10^6$  to  $10^7$  sweeps.

To speed up simulations, the QPS interaction in Eq. (23) is precalculated on a fine grid and stored in a look-up table. This enables quick on the fly evaluation by bilinearly interpolating to the continuous vortex positions.

The tunneling amplitudes  $t_m$  are readily calculated from the histograms of the net topological charge  $m$  of the instanton configurations. An important technical detail here, is that the exact formula Eq. (38) for the QPS amplitude proves to be quite sensitive to statistical noise, especially deep in the superconducting phase when  $t_m \ll \Delta_0$ . In those situations, we employ an alternative method of calculating  $t_1$ . We extract it from the effective capacitance, or equivalently from the variance of the distribution  $P_m$  of net instanton number. This variance  $\langle m^2 \rangle$  is simply

$$\langle m^2 \rangle = -\frac{\partial^2}{\partial k^2} \langle e^{ikm} \rangle \Big|_{k=0} = \beta \sum_{m=1}^{\infty} 2t_m m^2. \quad (48)$$

Assuming  $t_1$  dominates the sum, one may approximate it as  $t_1 \approx \langle m^2 \rangle / 2\beta$ . Although this estimate of  $t_1$  is not exact other than in the dilute limit, the distribution often fits nicely to the dilute form  $P_m = e^{-\sigma^2} I_m(\sigma^2)$  ( $I_m$  is an  $m^{\text{th}}$  order modified Bessel function and  $\sigma = \langle m^2 \rangle$ ), even for quite high QPS densities. We conclude that the variance should give a reasonable estimate of  $t_1$  also in that case.

The tunneling amplitudes  $t_m$  are, strictly speaking, ground state properties of the model and thus require extrapolation to zero temperature. All our simulations are carried out in the low-temperature limit  $\beta \gtrsim L/c_0$ , where  $t_m$  quickly approaches its zero-temperature limit. The quantities  $E_k$ ,  $V_k$ , and  $C_k$ , which give the response of the wire to an imposed charge displacement, are meaningful also at nonzero temperature, although we have not systematically investigated their temperature dependence.

## V. RESULTS AND DISCUSSION

### A. QPS amplitude

A main issue in the field has been the nature of the breakdown of superconductivity in MoGe nanowires. Early empirical evidence pointed in the direction of a quantum superconductor-insulator transition governed by whether the total normal resistance  $R_N$  of the wire is smaller or larger than the resistance quantum  $R_Q$ ,<sup>1</sup> similar to what happens in a single Josephson junction shunted by a normal resistance.<sup>34,35</sup> However, later experiments<sup>2,3</sup>

suggested that a better control parameter was the wire cross section area  $s$  (proportional to  $L/R_N$ ), at least for wires of length  $L \gg 200$  nm. This is in agreement with the notion that the action for one QPS  $S_0 = S_{\text{core}} + \frac{1}{2}V_0$  is the main parameter that determines the phase boundary. As discussed above, this is really a crossover, but since the dependence is exponential it becomes quite sharp.

Considering this, we plot in Fig. 3 the phase slip amplitude in the dilute instanton limit, Eq. (44), in the plane of  $L/R_N$  vs  $L$ . The phase slip amplitude is in this limit mainly determined by the self-interaction  $V_0$ , and the core action  $S_{\text{core}}$ , included in a chemical potential as

$$\mu = \ln y = \ln(S_{\text{core}}) - S_{\text{core}}. \quad (49)$$

Including the effects of interactions between phase slips through MC simulations, the result is that of Fig. 4. The phase slip amplitude is now significantly suppressed for long wires and low  $L/R_N$  compared to the dilute case, but on a qualitative level the two contour plots are quite similar. [Figure 3 displays a nonmonotonic behavior as function of  $L/R_N$ , which is absent in the simulation results shown in Fig. 4. This is due to the prefactor in Eq. (44) and only occurs in the regime of relatively high QPS amplitude, where the validity of the dilute limit is highly questionable.] In both cases, we take the correlation length  $\xi = 10$  nm and the critical temperature  $T_c = 5$  K ( $\Delta_0 = 1.76k_B T_c$ ), values typical for MoGe wires,<sup>36</sup> and also assume a capacitance of  $C \approx 5$  pF/m. The difference between  $t_1^{\text{DL}}$  and  $t_1$  is best seen in Fig. 5, which shows the same data of  $t_1^{\text{DL}}$  and  $t_1$  vs  $L/R_N$ , for three different fixed wire lengths  $L = 100, 300$ , and  $600$  nm. The dilute instanton gas approximation consistently overestimates  $t_1$ , but as expected, when the QPS amplitude diminishes for larger  $L/R_N$ , it becomes better and better.

The contour plots in Figs. 3 and 4 mark the crossover from rare to frequent QPS, which in practice defines the phase boundary for the superconductor-insulator transition detected in experiments. Our results are in qualitative agreement with the experiments of Ref. 3: A steep increase close to  $R = R_Q$  (the dashed white line in Figs. 3 and 4) for short wires, which then flattens out to a more or less horizontal line  $L/R_N = \text{const.}$  for longer wires.

### B. Phase slip interaction effects

Interactions are important both near the superconductor-insulator transition and in the region of strong coherent QPS. The signatures of a BKT transition will be most clear in the case of a purely linear dispersion (see Eq. (17)), which is formally obtained by taking  $\lambda \ll \xi$ , since this gives a purely logarithmic QPS interaction. In Fig. 6, we plot the phase diagram in this limit, as functions of  $K$  and  $\mu = \ln y$ . [A similar phase diagram is obtained in the case of Josephson junction chains, but with  $K = \sqrt{E_J/E_{C_0}}$ ,  $\lambda = \sqrt{C/C_0}$ , and  $\mu \sim -\sqrt{E_J/E_C}$ .] At the transition  $t_1 \sim L^{-1}$ , as discussed in Sec. IIID, and this is used to locate



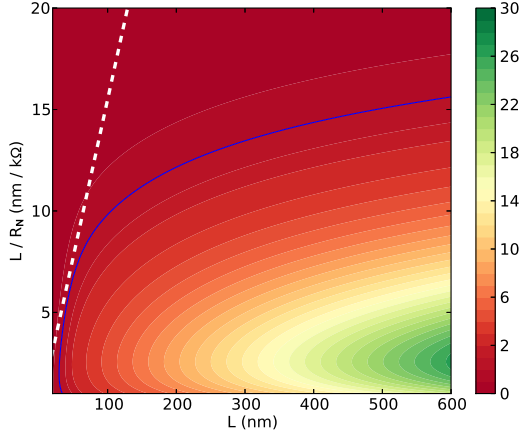


FIG. 3. (Color online) The QPS amplitude  $t_1^{\text{DL}}$ , in the dilute instanton limit, in the plane of  $L/R_N$  vs  $L$ . The QPS amplitude is measured in units of  $\Delta_0$ . The white dashed line is the line  $R_N = R_Q$ , and the blue line marks the contour  $t_1 = \Delta_0$ . (Assuming  $\xi = 10$  nm,  $\Delta_0 = 1.76k_B T_c$  (from BCS) with  $T_c = 5$  K, and  $C \approx 5$  pF/m.)

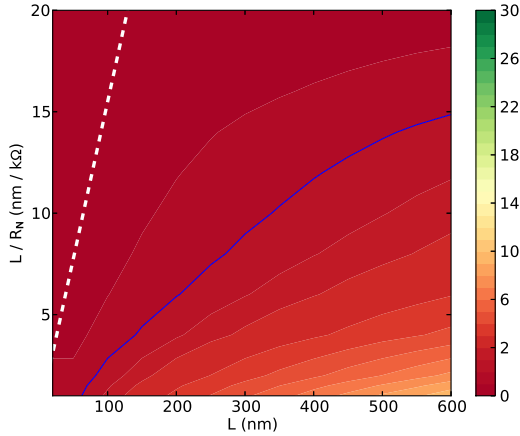


FIG. 4. (Color online) The QPS amplitude  $t_1$ , from simulations, in the plane of  $L/R_N$  vs  $L$ . The QPS amplitude is measured in units of  $\Delta_0$ . The white dashed line is the line  $R_N = R_Q$ , the blue line  $t_1 = \Delta_0$ .

the transition as the parameter values where  $Lt_1$  is independent of  $L$ , as shown in the inset. The phase boundary is nearly vertical for small  $\mu$  (large  $S_{\text{core}}$ ), where  $K$  remains largely unrenormalized.<sup>37</sup> Screening of the QPS interaction then renormalizes  $K$  towards higher values when  $\mu$  increases, reflected by the bending of the phase boundary above  $\mu \approx -5$ .

Note that the overall magnitude of  $t_1$  is strongly suppressed when  $\lambda \gg \xi$  in the regime near the SI transition, since the QPS action  $S_0 \sim K\lambda/\xi \gg 1$ , when  $K \gtrsim 2/\pi$ . The phase boundary observed in experiments on wires,

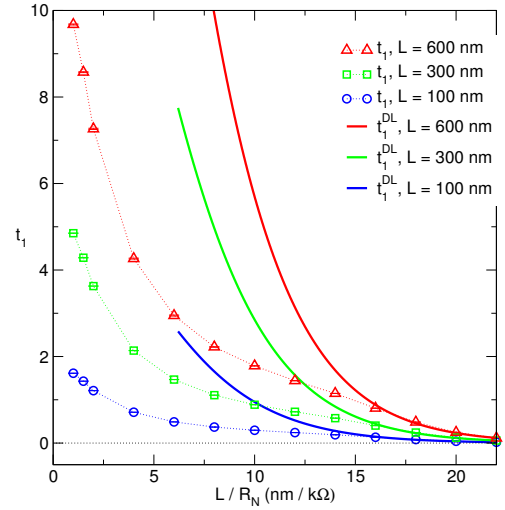


FIG. 5. (Color online) The QPS amplitude  $t_1$  (from simulations) and  $t_1^{\text{DL}}$  (from the dilute instanton limit) vs  $L/R_N$  for fixed  $L = 100, 300$ , and  $600$  nm. The QPS amplitude is measured in units of  $\Delta_0$ .

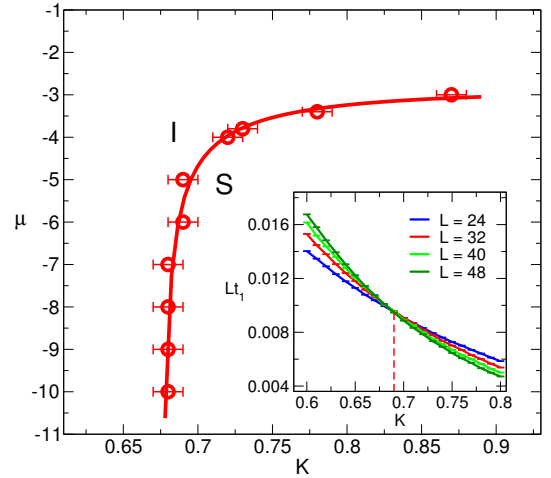


FIG. 6. (Color online) A phase diagram of the model in the limit  $\lambda \ll x_0 \ll L$  ( $\lambda = 0.001$ ,  $x_0 = 1$ ), in the coupling constant  $\bar{K}$  and the chemical potential  $\mu$  plane. The  $\bar{K}_c$  curve is constructed from the intersection of  $Lt_1$  vs  $\bar{K}$  curves for  $L, \beta = 24, 32, 40$ , and  $48$ . The letter S marks the superconducting phase, and I the insulating phase. Inset: Example of the scaled phase slip amplitude  $Lt_1$  vs  $K$  for different  $L$  intersecting at  $K \approx 0.68$  for  $\mu = -8$ .

whose length is smaller than or comparable to  $\lambda$ , is therefore more likely a crossover between low and high QPS amplitudes, at much lower  $K$ .

Effects of interactions are perhaps easier to observe in the regime of coherent QPS. As discussed in Sec. III C, the response of the wire to an applied charge displacement  $k$  is, in the noninteracting limit, governed by simple cosine or sine behaviors in  $E_k$ ,  $V_k$ , and  $C_k^{-1}$ . Any deviations from these forms are in this sense a sign of interactions

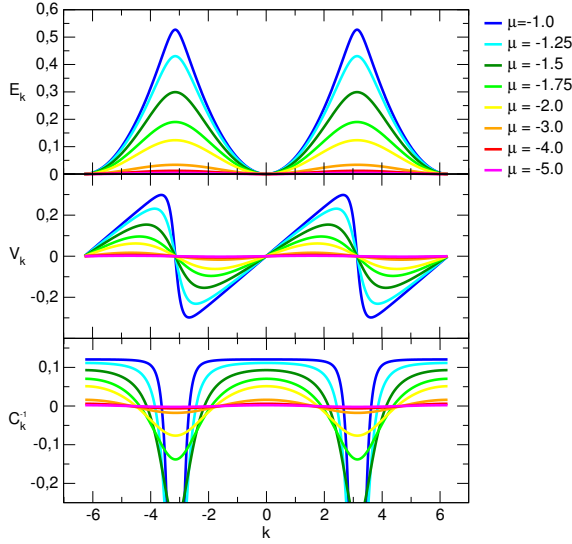


FIG. 7. (Color online)  $E_k$ ,  $V_k$ , and  $C_k^{-1}$  for different  $\mu$  at  $\lambda/x_0 = 20$  and  $K = 0.3$ . System size is  $10x_0 \times 10\tau_0$ .

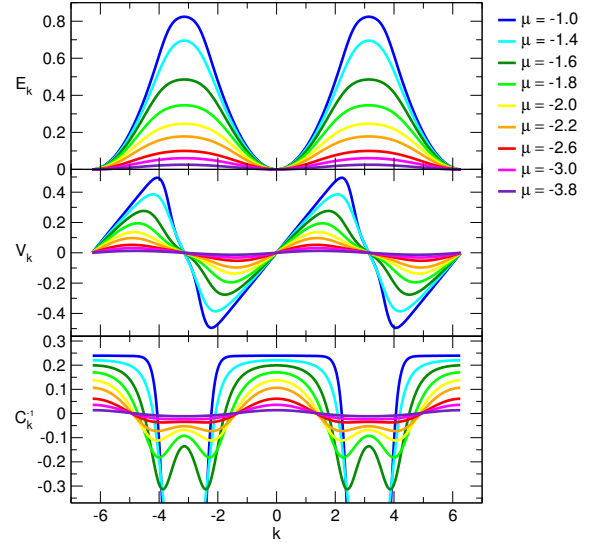


FIG. 9. (Color online)  $E_k$ ,  $V_k$ , and  $C_k^{-1}$  for different  $\mu$  at  $\lambda/x_0 = 1$  and  $K = 1$ . System size is  $10x_0 \times 10\tau_0$ .

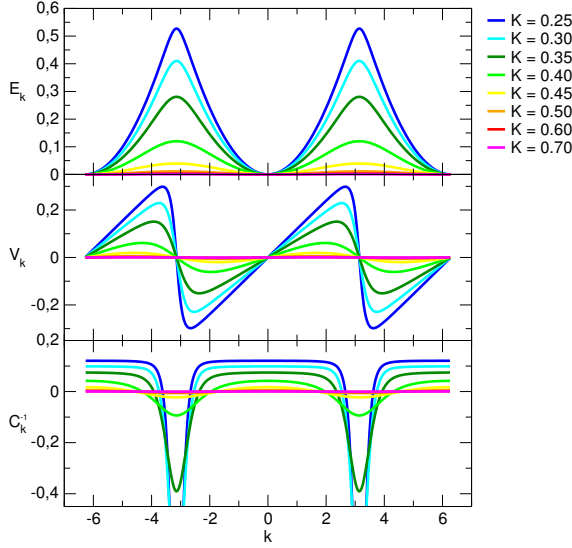


FIG. 8. (Color online)  $E_k$ ,  $V_k = dE_k/dk$ , and  $C_k^{-1} = d^2E_k/dk^2$  for different  $K$  at  $\lambda/x_0 = 20$  and  $\mu = -1$ . System size is  $10x_0 \times 10\tau_0$ .

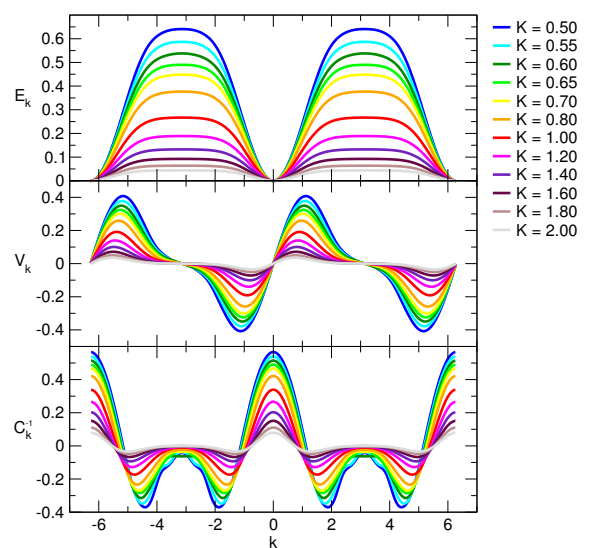


FIG. 10. (Color online)  $E_k$ ,  $V_k$ , and  $C_k^{-1}$  for different  $K$  at  $\lambda/x_0 = 0.001$  and  $\mu = -3$ . System size is  $10x_0 \times 10\tau_0$ .

between QPS.

In Fig. 7 curves of  $E_k$ ,  $V_k$ , and  $C_k^{-1}$  from simulations in the limit ( $\lambda/x_0 \gg 1$ ), show how these quantities change from sinusoidal to distinctly different shapes, as the chemical potential  $\mu$  increases, and thus the density of QPS increases. At the higher densities,  $E_k$  approaches a pattern of crossing parabolas with a period of  $2\pi$  (corresponding to charge transfers of  $2e$  Cooper pairs), indicative of a situation with a wildly fluctuating superconducting phase and a well defined charge variable, conjugate to the phase. Here, the low energy excitations of the wire are dominated by a capacitive energy, quadratic in the charge

displacement  $k$ . The maximum of the sawtooth-like  $V_k$  curves, tells us what voltage is required to push a Cooper pair through the wire, i.e., the threshold voltage it takes to overcome the Coulomb blockade in this phase. Further, the inverse of the effective capacitance  $C_k^{-1}$  increases steadily for higher densities of QPS (larger  $\mu$ ), as can be seen in the bottom panel of Fig. 7, until it reaches the limiting value  $L/(C\lambda^2)$ .

An almost identical evolution of the shapes of the energy, voltage, and inverse capacitance vs  $k$  can be seen in Fig. 8, where instead the coupling constant  $K$  is varied and the chemical potential  $\mu = -1$  is kept constant, but

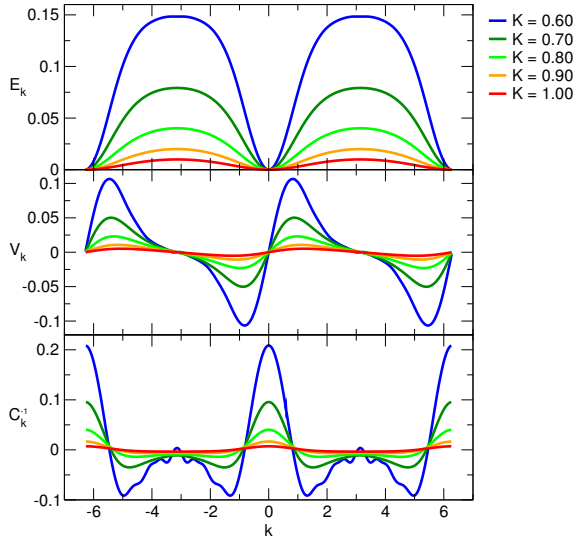


FIG. 11. (Color online)  $E_k$ ,  $V_k$ , and  $C_k^{-1}$  for different  $K$  at  $\lambda/x_0 = 1$  and  $\mu = -3$ , for a system of size  $40x_0 \times 40\tau_0$ . The small scale oscillations are due to statistical noise in the simulation.

with the same effect of changing the phase slip density (small  $K$  corresponds to high phase slip density and vice versa).

Focusing on the case of a shorter charge screening length  $\lambda$ , the curves can take on more exotic shapes than discussed previously. In Fig. 9, which displays simulation results for  $\lambda/x_0 = 1$  and  $K = 1$  while varying  $\mu$ , the crossing of the parabolas in  $E_k$  from above are now distinctly more rounded and somewhat flattened, giving the  $V_k$  sawtooth curves a backward tilt. This trend is even more pronounced in Fig. 10, where the charge screening length is even smaller,  $\lambda/x_0 = 0.001$  and the chemical potential  $\mu = -3$ . A similar behavior can be obtained by keeping  $\lambda$  fixed and going to larger system sizes, so that  $\lambda$  is still much smaller than  $L$ . An example of this can be seen in Fig. 11, where  $\lambda/x_0 = 1$  and  $L = 40x_0$ . These peculiar shapes can be understood by a simple argument: as the charge displacement  $ek/\pi$  increases from zero, a pair of positive and negative Cooper pairs is created and dragged apart leading to an initial steep rise of the energy. As the separation becomes comparable to the charge screening length  $\lambda$ , i.e., when  $k \gtrsim 2\pi\lambda/L$ , the attractive interaction will start to level off and eventually flatten out since there is no extra energy required to separate the pair further.

## VI. CONCLUSIONS

We have constructed a framework for modeling and simulations of quantum phase slips, based on a micro-

scopic model of a superconducting ultrathin wire. The low-energy effective action<sup>10,11</sup> is transformed, first, into a charge-current model and then to a gas of interacting instantons. Our treatment differs from most earlier works by the inclusion of electromagnetic fluctuations, thus enabling the tunneling of flux quanta across the wire, between the otherwise degenerate flux states.

With this we are able to calculate, via Monte Carlo simulations, the QPS tunneling amplitude beyond the dilute instanton gas approximation, without any restriction of the QPS density, and study the effects of instanton interactions. The regime of validity of the noninteracting instanton gas approximation is found to be limited to quite low densities, see Fig. 5.

By tuning the QPS action  $S_0$  and coupling constant  $K$  (both dependent on the thickness  $s$  of the wire), it is possible to go from a superconducting state with few incoherent QPS to an insulating state with coherent QPS. In the coherent regime, the linear response to an applied voltage is capacitive. Only when the voltage exceeds a certain threshold voltage will current start to flow. We have calculated the corresponding voltage-charge displacement relation  $V(k)$  and the effective (inverse) quantum capacitance  $C^{-1}(k)$  of the whole wire. These change from simple sinusoidal relations at low QPS density into sawtooth and other nontrivial shapes as the density increases and hence interactions become more important.

Circuits operating in the coherent regime will in many respects be dual to superconducting ones.<sup>6</sup> For example, an applied constant current  $I = (e/\pi)dk/dt$  would lead to Bloch oscillations,<sup>38</sup> i.e., an oscillating voltage with frequency  $\nu = I/2e$ , which holds the promise of defining an electric current standard, which is currently lacking. One may speculate that frequency locking of the oscillations and the observation of dual Shapiro steps could be facilitated by tuning the shape of the  $V(k)$  curves. Experimental efforts to realize devices based on QPS are under development.<sup>39,40</sup> A Cooper pair transistor device dual to the dc SQUID was recently suggested,<sup>39</sup> which might admit experimental studies of the voltage-charge relations calculated above.

The calculational methods developed here lays the foundations for future quantitative studies of the influence of disorder, dissipation, and temperature in superconducting nanowires and more complicated structures and devices.

## ACKNOWLEDGMENTS

Discussions with T. H. Hansson and D. Haviland are gratefully acknowledged. The simulations were performed on resources provided by the Swedish National Infrastructure for Computing (SNIC) at PDC Centre for High Performance Computing (PDC-HPC).

\* jlidmar@kth.se

<sup>1</sup> A. Bezryadin, C. Lau, and M. Tinkham, *Nature* **404**, 971 (2000).

- <sup>2</sup> C. N. Lau, N. Markovic, M. Bockrath, A. Bezryadin, and M. Tinkham, Phys. Rev. Lett. **87**, 217003 (2001).
- <sup>3</sup> A. T. Bollinger, R. C. Dinsmore, A. Rogachev, and A. Bezryadin, Phys. Rev. Lett. **101**, 227003 (2008).
- <sup>4</sup> I. M. Pop, I. Protopopov, F. Lecocq, Z. Peng, B. Pannetier, O. Buisson, and W. Guichard, Nature Physics **6**, 589 (2010).
- <sup>5</sup> K. Y. Arutyunov, T. T. Hongisto, J. S. Lehtinen, L. I. Leino, and A. L. Vasiliev, Scientific reports **2**, 293 (2012).
- <sup>6</sup> J. E. Mooij and Y. V. Nazarov, Nature Physics **2**, 169 (2006).
- <sup>7</sup> O. V. Astafiev, L. B. Ioffe, S. Kafanov, Y. A. Pashkin, K. Y. Arutyunov, D. Shahar, O. Cohen, and J. S. Tsai, Nature **484**, 355 (2012).
- <sup>8</sup> J. T. Peltonen, O. V. Astafiev, Y. P. Korneeva, B. M. Voronov, A. A. Korneev, I. M. Charaev, A. V. Semenov, G. N. Golt'sman, L. B. Ioffe, T. M. Klapwijk, and J. S. Tsai, Physical Review B **88**, 220506 (2013).
- <sup>9</sup> V. E. Manucharyan, N. A. Masluk, A. Kamal, J. Koch, L. I. Glazman, and M. H. Devoret, Phys. Rev. B **85**, 024521 (2012).
- <sup>10</sup> D. S. Golubev and A. D. Zaikin, Phys. Rev. B **64**, 014504 (2001).
- <sup>11</sup> K. Arutyunov, D. Golubev, and A. Zaikin, Physics Reports **464**, 1 (2008).
- <sup>12</sup> K. A. Matveev, A. I. Larkin, and L. I. Glazman, Physical Review Letters **89**, 096802 (2002).
- <sup>13</sup> G. Rastelli, I. M. Pop, and F. W. J. Hekking, Physical Review B **87**, 174513 (2013).
- <sup>14</sup> R. Fazio and H. Van Der Zant, Physics Reports **355**, 235 (2002).
- <sup>15</sup> A. Ergül, J. Lidmar, J. Johansson, Y. Azizoğlu, D. Schaeffer, and D. B. Haviland, New Journal of Physics **15**, 095014 (2013).
- <sup>16</sup> M. Feigel'man, L. Ioffe, V. Kravtsov, and E. Cuevas, Annals of Physics **325**, 1390 (2010).
- <sup>17</sup> S. Sachdev, P. Werner, and M. Troyer, Physical Review Letters **92**, 237003 (2004); A. Del Maestro, B. Rosenow, and S. Sachdev, Annals of Physics **324**, 523 (2009).
- <sup>18</sup> J. E. Mooij and C. J. P. M. Harmans, New Journal of Physics **7**, 219 (2005).
- <sup>19</sup> A. G. Semenov and A. D. Zaikin, Physical Review B **88**, 054505 (2013).
- <sup>20</sup> J. E. Mooij and G. Schön, Phys. Rev. Lett. **55**, 114 (1985).
- <sup>21</sup> A. Vestergren, J. Lidmar, and T. H. Hansson, Europhysics Letters (EPL) **69**, 256 (2005).
- <sup>22</sup> A. Vestergren and J. Lidmar, Physical Review B **72**, 174515 (2005).
- <sup>23</sup> T. Weißl, G. Rastelli, I. Matei, I. M. Pop, O. Buisson, F. W. J. Hekking, and W. Guichard, Phys. Rev. B **91**, 014507 (2015).
- <sup>24</sup> A. D. Zaikin, D. S. Golubev, A. van Otterlo, and G. T. Zimányi, Phys. Rev. Lett. **78**, 1552 (1997).
- <sup>25</sup> G. Refael, E. Demler, Y. Oreg, and D. S. Fisher, Phys. Rev. B **75**, 014522 (2007).
- <sup>26</sup> G. Refael, E. Demler, and Y. Oreg, Phys. Rev. B **79**, 094524 (2009).
- <sup>27</sup> R. M. Bradley and S. Doniach, Phys. Rev. B **30**, 1138 (1984).
- <sup>28</sup> E. Chow, P. Delsing, and D. B. Haviland, Phys. Rev. Lett. **81**, 204 (1998).
- <sup>29</sup> V. S. Berezinskii, Sov. Phys. JETP **32**, 493 (1971), [Zh. Eksp. Teor. Fiz. **59**, 907 (1970)]; J. M. Kosterlitz and D. J. Thouless, J. Phys. C **6**, 1181 (1973).
- <sup>30</sup> S. L. Sondhi, S. M. Girvin, J. P. Carini, and D. Shahar, Reviews of Modern Physics **69**, 315 (1997).
- <sup>31</sup> A. Andersson and J. Lidmar, Physical Review B **87**, 224506 (2013).
- <sup>32</sup> J. Lidmar and M. Wallin, Phys. Rev. B **55**, 522 (1997).
- <sup>33</sup> J. P. Valleau and L. K. Cohen, J. Chem. Phys. **72**, 5935 (1980).
- <sup>34</sup> S. Chakravarty, Phys. Rev. Lett. **49**, 681 (1982).
- <sup>35</sup> A. Schmid, Phys. Rev. Lett. **51**, 1506 (1983).
- <sup>36</sup> A. Bezryadin, J. Phys.: Cond. Mat. **20**, 043202 (2008).
- <sup>37</sup> The critical  $K$  obtained is slightly higher than the expected  $2/\pi$ , due to subleading corrections to the asymptotic logarithmic  $L$  dependence in Eq. (27).
- <sup>38</sup> J. S. Lehtinen, K. Zakharov, and K. Y. Arutyunov, Phys. Rev. Lett. **109**, 187001 (2012).
- <sup>39</sup> T. T. Hongisto and A. B. Zorin, Phys. Rev. Lett. **108**, 097001 (2012).
- <sup>40</sup> A. M. Hriscu and Y. V. Nazarov, Phys. Rev. B **83**, 174511 (2011).